JCE

Journal of Civil Engineering
ISSN 2086 - 1206 E-ISSN 2579 - 9029

Enhancement of Flood Hazard Assessment through Parameters Modification: A Case Study of the Sikambing Watershed

Fiqih J. Fachri[ac*], Dhemi Harlan[b], Joko Nugroho[b], Ana N. Chaidar[b], Muh. Reysha S. Kasim[a]

Correspondence

[a]Water Resources Management, Bandung Institute of Technology, ITB Ganesha Campus , Bandung 40132, Indonesia.
[b]Water Resources Engineering Research Group, Bandung Institute of Technology, ITB Ganesha Campus , Bandung 40132, Indonesia.
[c]Directorate General of Water Resources, Ministry of Public Works, South Jakarta 12110, Indonesia.

Corresponding author email adress: fiqih.julfachri@pu.go.id

Submitted : 03 January 2025
Revised : 06 February 2025
Accepted : 18 February 2025

Abstract

This study focuses on enhancing the flood hazard assessment parameters in Indonesia, particularly within the framework established by the National Disaster Management Agency (NDMA) of the Republic of Indonesia. Given the multifaceted nature of flood hazards, influenced by factors such as land cover change, climate change, and the failure of flood control structures, it is essential to adopt a more comprehensive approach to flood hazard assessment. The research was conducted in the Sikambing Watershed in Medan City, North Sumatra Province, an area that has experienced 12 significant flood events affecting over 13,000 individuals between 2020 and 2024. To improve the flood hazard assessment, this study employs a quantitative method where hydrological and hydraulic analyses serve as the empirical foundation, and flood hazard mapping is carried out by modifying existing parameters to incorporate flood depth (d), flow depth and velocity (dv), and flood duration (T). Additionally, a comparison is made with the flood hazard map based on NDMA parameters to analyze the changes in hazard classification. The resulting flood hazard map indicates a total inundated area of 227.65 hectares; however, the use of different parameters results in significant changes in the proportions of each hazard class. While the low classification dominates both maps, there is an increase in the inundated area classified as medium, covering 17.43 hectares, compared to only 3.25 hectares for the medium hazard classification in the NDMA-based flood hazard map. These results demonstrate that parameter modification provides a more comprehensive picture of flood hazard assessment. This research is expected to contribute to disaster mitigation planning, evacuation strategies and the development of more effective flood control infrastructure.

Keywords

Flood hazard assessment, disaster management, flood risk mitigation

INTRODUCTION

Referring to the policies in Indonesia related to disaster management, one of the key aspects is the need to establish sustainable disaster risk governance [1]. Every year, the National Disaster Management Agency of the Republic of Indonesia (NDMA) measures the level of disaster risk in each region of Indonesia through the Indonesia Disaster Risk Index (IDRI). The disaster risk assessment conducted by NDMA includes the components of hazard, vulnerability, and capacity [2]. The hazard component is evaluated based on spatial probability, frequency of occurrence, and the intensity of natural phenomena. However, according to NDMA, the hazard component is the most challenging element to minimize. This is due to the ongoing trend of increasing impacts of hazards each year, leading to the assumption that the hazard component remains constant in accordance with the baseline conditions established in the Indonesia Disaster Risk Index (IDRI) of 2013.

On the other hand, flood hazards have several contributing factors, one of which is land cover change [3]. More complex causes include the overflow of water at the river mouth due to rising sea levels caused by wind, waves, and tidal surges, which obstruct river flow and elevate water levels during storms [4], flooding can also be caused by climate change [5], [6], [7], or due to the failure of flood control structures [8], [9]. Therefore, the assessment of flood hazards should not be a constant evaluation to be established within the disaster risk index component.

The assessment of flood hazards can be conducted by considering hydrological analysis and hydrodynamic modeling at a specific flood study location [10], [11]. This method is referred to as quantitative assessment because it requires hydrodynamic modeling of the flooding process to calculate the spatial distribution of flood hazard indicators that accurately reflect the intensity and frequency of floods, thereby indicating the potential hazards that may arise [12].

NDMA defines flood hazard indicators solely based on flood depth parameters, which are categorized into three classifications. The low classification is designated for flood depths of less than 0.76 m, while the medium

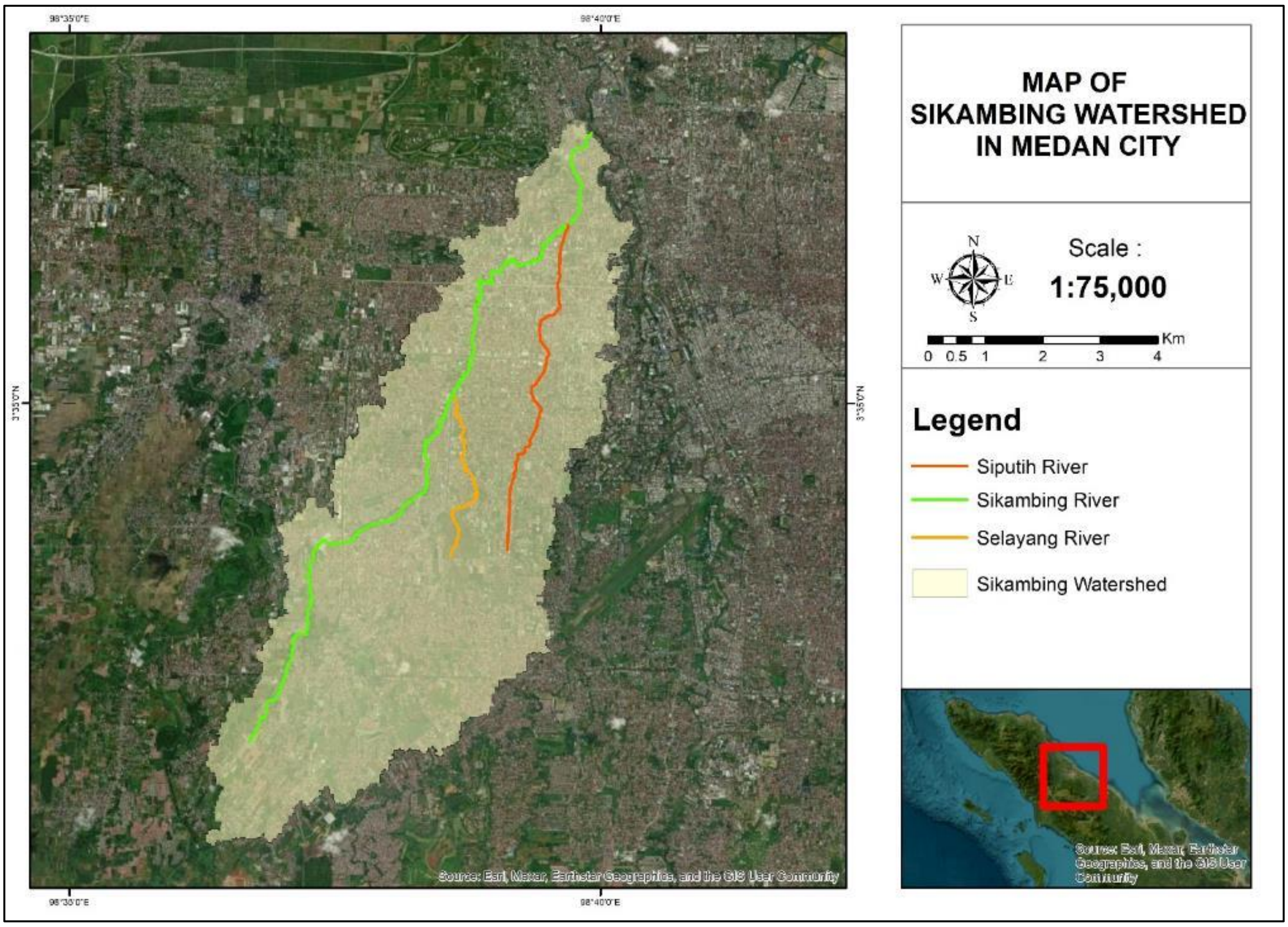

Figure 1 Sikambing watershed

classification encompasses flood depths ranging from 0.76 m to 1.5 m, and the high classification is assigned to flood depths exceeding 1.5 m [13]. Based on previous research and the policies of other countries, flood assessment should not only consider flood depth parameters but also combine several parameters, such as flood depth and flow velocity [8], [14], [15], [16], [17] or include flood duration as a relevant parameter in flood assessment [18], [19], [20].

In Indonesia, there are additional policies that regulate the parameters for determining priorities in flood management, which serve as a reference for urban drainage system planning [21]. The policy outlines the parameters used, which include flood depth, flood extent, flood duration, and flood frequency. Although there has been a review of the need for reliable methods and advancements in the context of flood risk management [22], there is still no international consensus on which parameters should be utilized. Researchers tend to examine flood hazard assessment parameters based on case studies that are considered relevant and representative of flood conditions at the occurrence sites. This approach underscores the importance of local context in determining the most appropriate parameters for flood hazard assessment, thereby enhancing accuracy and effectiveness in flood risk mitigation. To this end, the authors attempt to improve the flood hazard assessment parameters used by NDMA by modifying the assessment to incorporate flood depth (d), flood depth and flow velocity (dv), as well as flood duration (T), based on previous research and considering policies [21] that represent conditions in Indonesia.

This study will be tested in the Sikambing Watershed in Medan City, North Sumatra Province, where, during the period from 2020 to 2024, there have been 12 flood events affecting 13,657 individuals and inundating 1,289 houses [23].

The Sikambing Watershed is part of the Deli Watershed [24], [25], covering an area of 41.22 km² and located in the southern region of Medan City, North Sumatra Province. The Sikambing Watershed encompasses six sub-districts in Medan City, namely Medan Barat, Medan Helvetia, Medan Petisah, Medan Sunggal, Medan Baru, and Medan Selayang, and is characterized by a densely populated residential area, making it significantly impacted by flooding events. Within the Sikambing Watershed, there is a network of the Sikambing River that stretches 15.85 km and has two tributaries: the Selayang River, which is 3.69 km long, and the Siputih River, which is 6.35 km long. The downstream of the Sikambing River meets the Deli River, which is a first-order river in the Deli Watershed. The study area is shown in Figure 1.

RESEARCH SIGNIFICANCE

This study aims to enhance the flood hazard assessment in Indonesia, which has traditionally been based solely on depth parameters. By adding and modifying the flood hazard assessment parameters, it is expected that the sensitivity of the flood hazard evaluation can be improved. The parameters used in this assessment include flood depth (d), which poses potential risks to humans and structures; flow depth and velocity (dv), which can affect human stability during flood events; and flood duration (T), which also impacts human safety and infrastructure damage.

METHODOLOGY

Flood hazard assessment is a fundamental and critical step in flood disaster risk analysis [26], [27]. This process generates crucial information that supports decision-making in flood control planning and policy [14], [28], including zoning regulations in flood-prone areas, with the aim of reducing negative impacts on communities and the environment [29], [30]. This study focuses on calculating design discharge and developing hydraulic models to estimate relevant parameters in flood assessment, namely depth (d), flood depth and flow velocity (dv), as well as flood duration (T). The results of these estimates are used to assess the level of flood hazard, which then serves as a reference for stakeholders in designing evidence-based mitigation strategies. Important analyses conducted include hydrological analysis, flood analysis in hydraulic modeling, and the creation of flood hazard mapping based on flood hazard assessment parameters.

A. HYDROLOGICAL ANALYSIS

The hydrological analysis is conducted by determining the design discharge due to the unavailability of measured discharge data in the study area. The rainfall data used comes from three observation stations within the study area: the Meteorology, Climatology, and Geophysics Agency (MCGA) Region I Medan, the Deli Serdang Geophysical Station, and the Sibolangit Rainfall Station, covering the period from 2007 to 2023. This data is processed to form average rainfall data based on the influence of the Thiessen polygon for each rainfall station [31]. Subsequently, frequency analysis is performed using various probability distribution functions, including Log Normal, Gumbel, and Log Pearson Type III, to determine the design rainfall for different return periods. Each probability distribution is tested to identify the most suitable distribution. The selected design rainfall results are then distributed using the PSA 007 method over a duration of 6 hours [32].

By determining the soil classification of the study area from the Harmonized World Soil Database (HWSD) and the land cover data from 2022 provided by the Ministry of Environment and Forestry, the initial abstraction value (Ia), Curve Number (CN), and Potential Maximum Storage (S) are analyzed. Considering the previously determined duration and intensity, runoff calculations are then performed using the SCS CN method [33]. This runoff is subsequently transformed into design discharge using the Nakayasu Synthetic Unit Hydrograph (SUH) method, where the selection of this method is based on calibration results that compare the bankfull discharge of the Sikambing River, calculated from river geometry data, against the design discharge for a 2-year return period [34], and is simulated using numerical modeling [35]. The design discharge used is for a 100-year return period, based on the policy of the Ministry of Public Works, which states that flood control measures for provincial capitals and metropolitan cities should utilize design discharges with return periods of up to 100 years [25], [36].

B. HYDRAULIC MODEL

This study utilizes HEC-RAS version 6.5 software for 2D hydraulic modeling. This software is well-suited for simulating flood events [37]. Topographic data, which integrates the surface characteristics of the study area, is crucial for flood modeling and needs to be enhanced as it is a significant factor affecting the accuracy of flood modeling [38]. The Digital Elevation Model (DEM) used as topographic data is sourced from a topographic survey of the study area using Light Detection and Ranging (LiDAR) technology, which has proven to be accurate in spatial flow distribution within HEC-RAS 2D hydraulic modeling [39]. The next step in building the hydraulic model involves determining the type of mesh used to achieve optimal computational efficiency [40]. This is to support results with good accuracy while enhancing computational efficiency, as not all parts of the model need to be computed with the same time step. The Manning's n value for the floodplain is obtained based on land cover analysis, while for the river channel, it is based on instantaneous discharge measurements [41], which are then calibrated with HEC-RAS 2D model simulations [42]. The obtained Manning's n values are converted into a polygon shapefile for the study area and incorporated as Land Cover in Ras Mapper HEC-RAS 2D. The design discharge for a 100-year return period is input as the upstream boundary condition, and normal depth is used as the downstream boundary condition. Computational settings, including computation interval, hydrograph output interval, mapping output interval, and detail output interval, must be specified for the simulation [43]. For model stability, a simulation time step known as the Courant condition is applied [44], as indicated by Equation 1.

$$C = \frac{v\Delta T}{\Delta x} \leq 1.0 \; (with\; C_{max} = 3.0) \qquad (1)$$

where, C is the Courant number, v is the flood wave velocity (m/s), ΔT the computational time step (s), and Δx the average cell size (m) [39].

The simulation in the modeling is then conducted using unsteady flow analysis, which is solved using the Saint Venant equations (Equation 2) or the diffusion wave equations (Equations 3 and 4).

$$\frac{\partial \zeta}{\partial t} + \frac{\partial p}{\partial x} + \frac{\partial q}{\partial y} = 0 \qquad (2)$$

$$\frac{\partial p}{\partial t} + \frac{\partial}{\partial x}\left(\frac{p^2}{h}\right) + \frac{\partial}{\partial y}\left(\frac{pq}{h}\right) = a \qquad (3)$$

$with$;

$$a = -\frac{n^2 pg\sqrt{p^2+q^2}}{h^2} - gh\frac{\partial \zeta}{\partial x} + pf + \frac{\partial}{\rho \partial x}(h\tau_{xx}) + \frac{\partial}{\rho \partial y}(h\tau_{xy})$$

$$\frac{\partial q}{\partial t} + \frac{\partial}{\partial y}\left(\frac{q^2}{h}\right) + \frac{\partial}{\partial x}\left(\frac{pq}{h}\right) = b \qquad (4)$$

$with;$

$$b = -\frac{n^2 qg\sqrt{p^2+q^2}}{h^2} - gh\frac{\partial \zeta}{\partial y} + qf + \frac{\partial}{\rho \partial y}(h\tau_{yy}) + \frac{\partial}{\rho \partial x}(h\tau_{xy})$$

where, h is the water depth (m), p and q are the specific flow in the x and y direction (m^2s^{-1}), ζ is the surface elevation (m), g is the acceleration due to gravity (ms^{-2}), n is the Manning's Roughness coefficient ($m^{-1/3}s$), ρ is the water density (kg m^{-3}), τ_{xx}, τ_{yy}, and τ_{xy} are the components of the effective shear stress and f is the Coriolos (s^{-1}). When the diffusive wave is selected, the inertial terms of the momentuum equation are neglected [39], [45].

Subsequently, the simulation results will be validated against observational data from the study area to achieve accuracy in flood modeling analysis under design discharge conditions. This simulation will produce parameters such as flood depth (d), flow depth and velocity (dv), and flood event duration (T).

C. MODIFICATION OF FLOOD HAZARD ASSESSMENT

Parameters commonly used in analyzing flood hazards include flood depth [10], [27], [28], [46], [47], [48], [49], [50], [51], including studies conducted in Indonesia [2], as well as flow velocity [16], [52], [53]. Some studies even combine these two parameters into a single variable assessed within the flood hazard classification [14], [15], [17], [54]. Additionally, the duration of flooding is still considered relevant in flood hazard assessments [18], [19], [20]. The enhancement of flood assessment through the addition and modification of parameters is based on previous research approaches and policies issued by the Ministry of Public Works.

The review of flood depth conducted by Mani et al. (2014) considers depth parameters based on protection for individuals and structures. A depth greater than 0.2 m is considered risky for humans, while a depth exceeding 1.5 m poses a risk to buildings. This aligns with policies in Indonesia [21], which categorize priority handling of flood inundation within a range of 0.1 m to greater than 0.5 m. Considering both references, a flood depth range of 0.5 to 1.5 m is established as the threshold for average depth that poses risks to both humans and structures. Therefore, the proposed parameters for flood depth can be seen in Table 1.

Table 1 Flood depth parameter

Flood Depth (m)	Flood Hazard Classification	Flood Hazard Index
0 – 0,1	Very Low	0
0,1 – 0,5	Low	1
0,5 – 1,5	Medium	2
1,5 – 3,5	High	3
>3,5	Very High	4

NDMA has not yet defined the parameters of flood depth and flow velocity (dv) as assessed parameters in flood hazard assessments [2]. However, research in Indonesia has been conducted that incorporates both depth and velocity parameters (dv) in flood assessments [54]. This study also references Mani et al. (2014), who state that depth and velocity represent momentum, or the product of depth and flow velocity, which can determine human instability during flooding. Research by Silvestro et al. (2016) explains that the average threshold of human instability in floods is around 1.35 m²/s, distinguishing between an upper threshold classified as high and a lower threshold classified as low. Furthermore, Mani et al. (2014) classify dv values as follows: 0 – 0.3 m²/s as very low, 0.3 – 0.7 m²/s as low, 1.2 – 1.6 m²/s as high, and >1.6 m²/s as very high. Based on the determination of the average threshold of human instability in floods and the classification established, the proposed parameters for flood depth and flow velocity (dv) can be seen in Table 2.

Table 2 Flood depth and flow velocity parameter

Flood Depth x Flow Velocity (m²/s)	Flood Hazard Classification	Flood Hazard Index
0 – 0,3	Very Low	0
0,3 – 0,7	Low	1
0,7 – 1,35	Medium	2
1,35 – 1,6	High	3
>1,6	Very High	4

In the studies by Mani et al. (2014) and Tingsanchali and Promping (2022), a flood duration of 24 hours (1 day) is classified as very low, while flood durations exceeding 140 hours to over 175 hours (more than 5 days) are classified as high to very high. This classification indicates a significant range of flood durations in flood hazard assessments, where the safety of individuals and structures must be considered. In contrast, the research by Ongdas et al. (2020) classifies flood duration requiring special attention at a medium level, which falls within the range of 5 to 24 hours, while flood durations exceeding 72 hours (more than 3 days) are classified at a crisis level. This classification remains relevant to policies in Indonesia [21], which state that flood durations between 1 hour and greater than 8 hours require special attention. Considering these references, a flood duration range of 5 to 24 hours is established as the threshold for average duration that poses risks to both humans and structures. Therefore, by taking into account the duration range from 1 hour to greater than 72 hours, the proposed parameters for flood duration (T) can be seen in Table 3.

Table 3 Flood duration parameter

Flood Duration (hours)	Flood Hazard Classification	Flood Hazard Index
0 – 3	Very Low	0
3 – 5	Low	1
5 – 24	Medium	2
24 – 72	High	3
>72	Very High	4

To conduct a comprehensive flood hazard assessment, a combination of the three parameters previously described is utilized. The research on the development of flood hazard assessment involves the integration of these three parameters using a weighting scenario with the Analytic Hierarchy Process (AHP) based on field surveys and questionnaires [20]. Although this method is considered more representative in depicting actual field conditions, the time and resources required for field surveys and data collection through questionnaires are highly dependent on the size of the area and the number of people and structures affected by flooding. Therefore, while this approach can enhance the accuracy of flood hazard maps, challenges related to time and resources remain significant considerations in flood hazard assessment. Meanwhile, Mani et al. (2014) combined these three parameters based on previous research into nine groups of parameter combinations while still considering each parameter individually. Thus, based on this reference and the efficiency considerations in developing flood hazard maps, the proposed classification scheme for flood hazards is presented in Table 4.

Table 4 Flood hazard assessment based on combination of parameters

Combination of 3 Parameters	Flood Hazard Index	Flood Hazard Classification
0<d<0,1 and 0<dv<0,3 and 0<T<50	0	Very Low
0<d<0,1 and 0<dv<0,3 and T>50	1	Low
0,1<d<0,5 or 0,3<dv<0,7 and 0<T<25	1	Low
0,1<d<0,5 or 0,3<dv<0,7 and T>25	2	Medium
0,5<d<1,5 or 0,7<dv<1,35 and 0<T<25	2	Medium
0,5<d<1,5 or 0,7<dv<1,35 and T>25	3	High
1,5<d<3,5 or 1,35<dv<1,6 and 0<T<25	3	High
1,5<d<3,5 or 1,35<dv<1,6 and T>25	4	Very High
d>3,5 or dv>1,35 and T>0	4	Very High

D. FLOOD ASSESSMENT BASED ON THE NATIONAL DISASTER MANAGEMENT AGENCY (NDMA)

To analyze the results of the flood hazard assessment based on parameter modifications, a comparison is made against the flood hazard assessment conducted by the NDMA. The flood hazard assessment by the NDMA is based on the depth parameter, which is divided into three classifications: low, medium, and high, as shown in the Table 5.

E. FLOOD HAZARD MAP

Flood hazard maps serve to provide information regarding the level of flood hazard in an area that experiences flooding events. From the results of hydraulic modeling using HEC-RAS 2D, a new calculated layer was created based on the classifications presented in Table 4 and Table 5, resulting in two distinct rasters: one representing the modified flood hazard assessment based on the combination of three parameters, and the other representing the depth spatial characteristics that reflect the NDMA flood assessment. These rasters were then processed using ArcGIS version 10.8 software to produce the flood hazard map.

Table 5 Flood assessment classification based on the NDMA

Flood Depth (m)	Flood Hazard Classification	Flood Hazard Index
< 0,76	Low	1
0,76 – 1,5	Medium	2
>1,5	High	3

RESULTS AND DISCUSSIONS

A. HYDROLOGICAL ANALYSIS RESULTS

In this study, the rainfall analysis in the Sikambing Watershed was conducted using the Thiessen polygon method to determine the influence of each rainfall station on the observed precipitation. Three rainfall stations were analyzed: the MCGA Regional I Medan Station, the Deli Serdang Geophysical Station, and the Sibolangit Rainfall Station, each showing different contributions to the formation of the Thiessen polygon. The MCGA Regional I Medan Station had an influence of 22.65%, while the Deli Serdang Geophysical Station contributed 27.30%. The Sibolangit Rainfall Station, with the highest influence, reached 50.05%. The results of these influences were then used to calculate the average annual maximum daily rainfall from the rainfall data collected from 2007 to 2023. The average annual maximum daily rainfall from 2007 to 2023 showed a significant variation, ranging from 39.17 mm to 113.81 mm. Through frequency analysis and testing, the Log Pearson Type III method was identified as the most suitable for planning rainfall. The analysis indicated a planned rainfall for a 100-year return period of 125.81 mm. This planned rainfall was then distributed with a PSA 007 value over 6 hours to establish the planned rainfall intensity.

Based on the results of land cover analysis and soil classification in the Sikambing Watershed, an Initial Abstraction (Ia) value of 8.31 mm was obtained, with a Curve Number (CN) calculated at 85.94, indicating a high potential for surface runoff due to the existing soil characteristics and land use. Additionally, a Potential Maximum Storage (S) value of 41.54 mm was determined. Using the SCS CN method, these three parameters were employed to calculate infiltration and runoff based on the previously analyzed planned rainfall. The runoff for the 100-year return period was found to be 86.81 mm. The runoff results were transformed using the Nakayasu Synthetic Unit Hydrograph (HSS) method, yielding a design discharge of 163.55 m^3/s for the 100-year return period.

Within the Sikambing River Network, there are two tributaries, namely the Selayang River and the Siputih River, which will also be modeled in HEC-RAS 2D to enhance the accuracy of flood analysis. Therefore, the design discharge for the 100-year return period in the Sikambing Watershed was divided into six sub-watersheds based on the delineation results from HEC HMS version 4.12, and the design discharge was modeled using this software to obtain the boundary conditions for flow discharge in each section of the Sikambing River and its

ISSN 2086 - 1206 E-ISSN 2579 - 9029

tributaries. The results of the watershed delineation are shown in Figure 2, and the design discharge as the upstream boundary condition for the six sub-watersheds is shown in Figure 3.

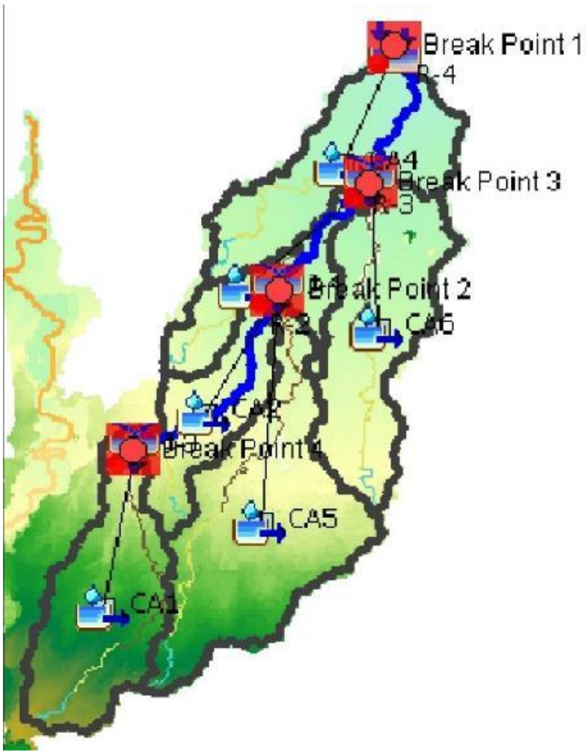

Figure 2 Delineation of the sikambing watershed

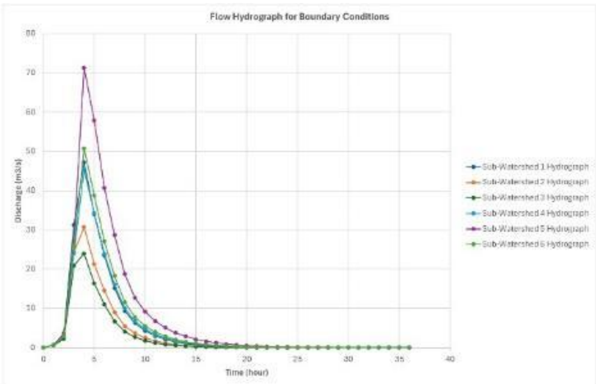

Figure 3 Hydrograph for boundary conditions

B. HYDRAULIC MODELING RESULTS

The Digital Elevation Model (DEM) data, sourced from topographic survey data using LiDAR technology, resulted in a high-resolution DEM with a grid size of 1 m. This outcome is highly favorable, as a smaller grid size can more accurately represent the floodplain surface. The DEM data was further enhanced by incorporating the geometric data of the Sikambing River and its tributaries, obtained from measurements, and was formatted to maintain the same resolution. Considering computational efficiency, the floodplain mesh was created with a size of 25 m, while the river network mesh was set at 3 m to achieve accuracy in flow modeling within the river network. From the land cover analysis of the Sikambing Watershed, it was found that 99.06% of the area is residential, leading to a Manning's n value of 0.05 for the floodplain. The Manning's n value for the river network was based on measurements of instantaneous discharge in the upstream, middle, and downstream segments of the Sikambing River. Using this observational data, the Manning's n value for the Sikambing River was determined to be 0.035.

An initial simulation was conducted to validate the model against flood events that occurred in the study area. During the recorded flood event, a discharge of 133.19 m³/s inundated six sub-districts: Medan Barat, Medan Helvetia, Medan Petisah, Medan Sunggal, Medan Baru, and Medan Selayang. The design discharge for a 25-year return period, calculated using the Nakayasu HSS method, was found to be 137.58 m³/s. This design discharge value approximates 96.70% of the recorded discharge; therefore, the design discharge for the 25-year return period will be used in the initial simulation for model validation. From the obtained observational data, no inundation area was recorded; however, flood events were identified at 14 locations within the six sub-districts, with recorded depth ranges from 0.2 m to 1 m. Consequently, the simulation results will be compared with the 14 flood event locations and the corresponding flood depths. The initial simulation results closely resembled the recorded flood event locations, with depth ranges from 0.2 m to 1.08 m, indicating that hydraulic modeling can be utilized for flood analysis at the 100-year return period discharge.

The results of the HEC-RAS 2D Simulation for a design discharge with a return period of 100 years, as shown in Figure 4, indicate that flood overflow predominantly occurs in the middle and downstream areas of the Sikambing River. In the Selayang River, flooding occurs almost along the entire length of the river, with the largest inundation areas located upstream and downstream. Meanwhile, the Siputih River also experiences flooding in its upstream and downstream sections, although the inundation area is relatively small compared to the other rivers. The results of this simulation were then processed to produce spatial raster with depth parameters (d) based on the NDMA, as shown in Figure 5, which was generated based on Table 5. Additionally, the spatial values that integrate the three parameters are illustrated in Figure 6, which was created based on Table 4.

C. FLOOD HAZARD MAP

Based on the flood depth parameters established by the National Disaster Management Agency (NDMA), a flood hazard map was created according to the results of the HEC-RAS 2D modeling, as shown in Figure 7. The flood hazard map indicates that at a design discharge with a return period of 100 years, the Sikambing Watershed experiences flooding over an area of 227.65 hectares, as classified in Table 6. The low classification is predominant, covering an area of 223.89 hectares, or 98.35% of the total inundated area, while the medium classification covers

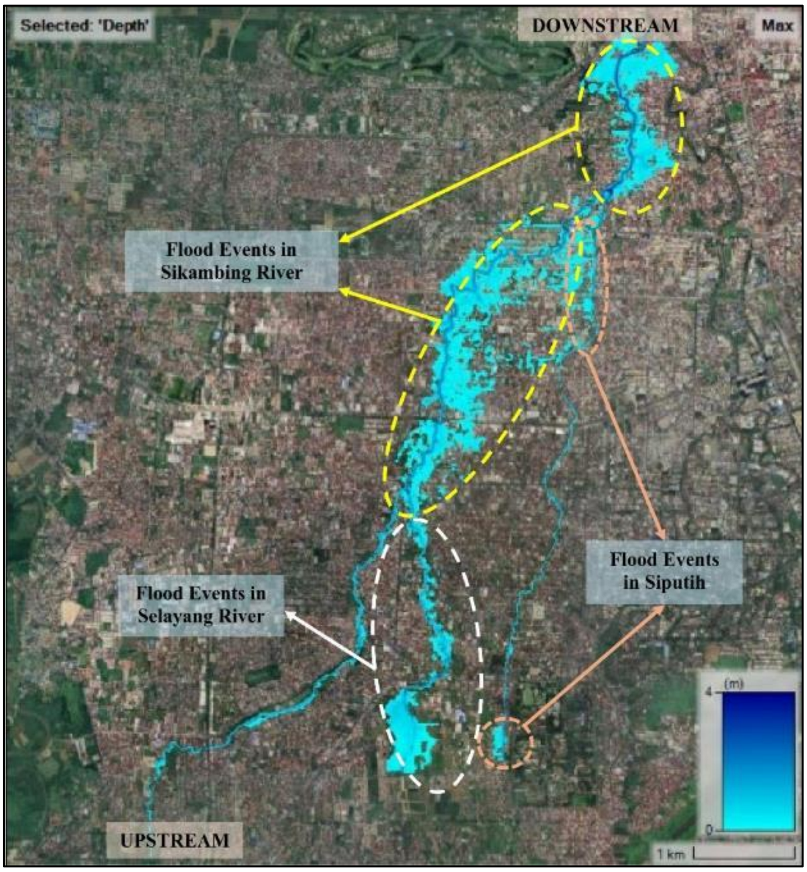

Figure 4 Result of the HEC-RAS 2D simulation

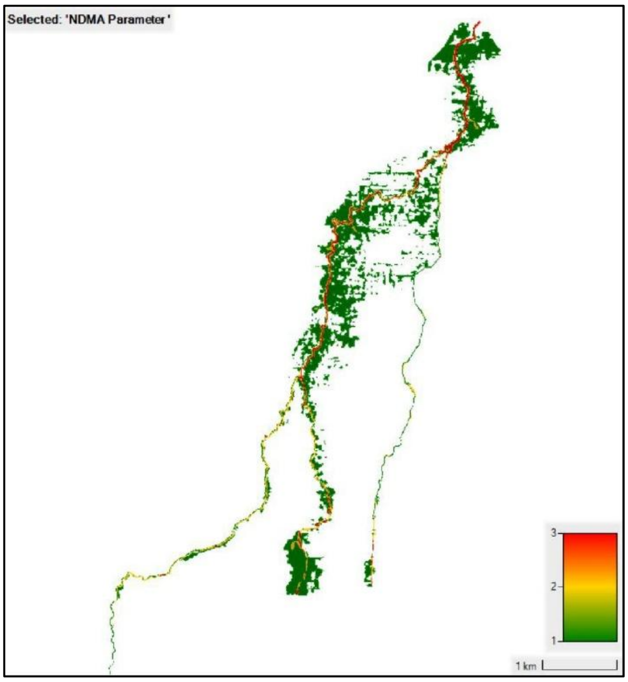

Figure 5 Raster based on NDMA parameter

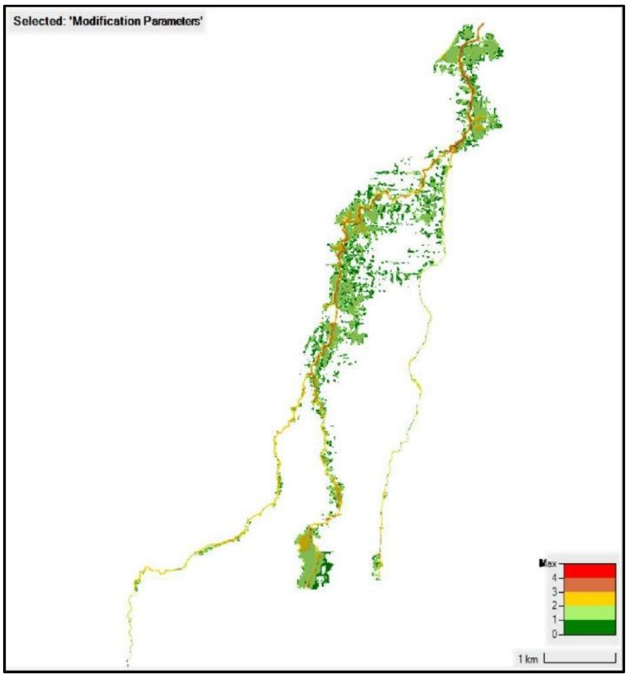

Figure 6 Raster based on modification parameters

3.25 hectares, representing only 1.43% of the total inundated area. The high classification shows a very small percentage of 0.23%, equivalent to only 0.52 hectares.

Furthermore, a flood hazard map was also developed based on the modified parameters. The results of the flood hazard map are illustrated in Figure 8, and the area of each classification is detailed in Table 7. The flood hazard classification for the Sikambing Watershed indicates that the very low and low classifications are the most dominant, comprising 29.98% and 62.32% of the total inundated area, respectively.

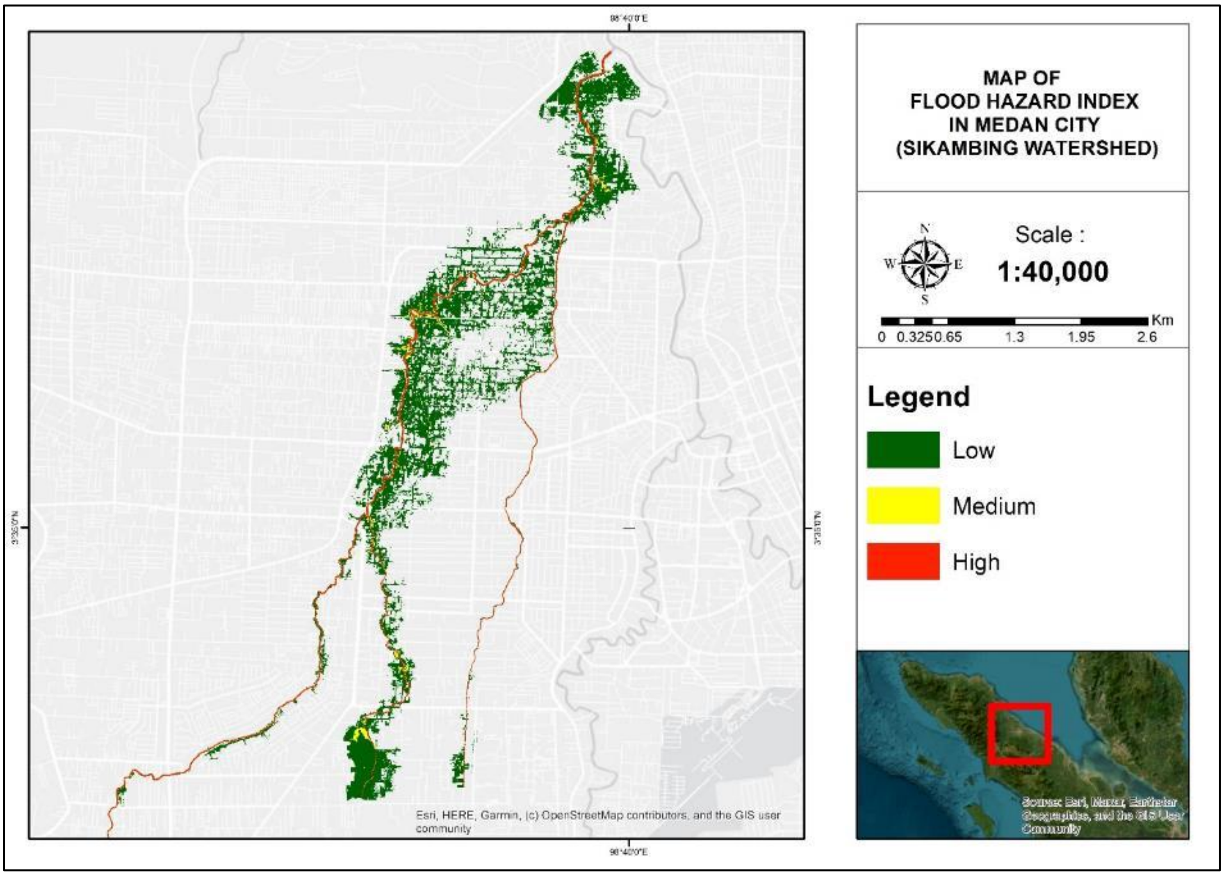

Figure 7 Flood hazard map based on NDMA parameter

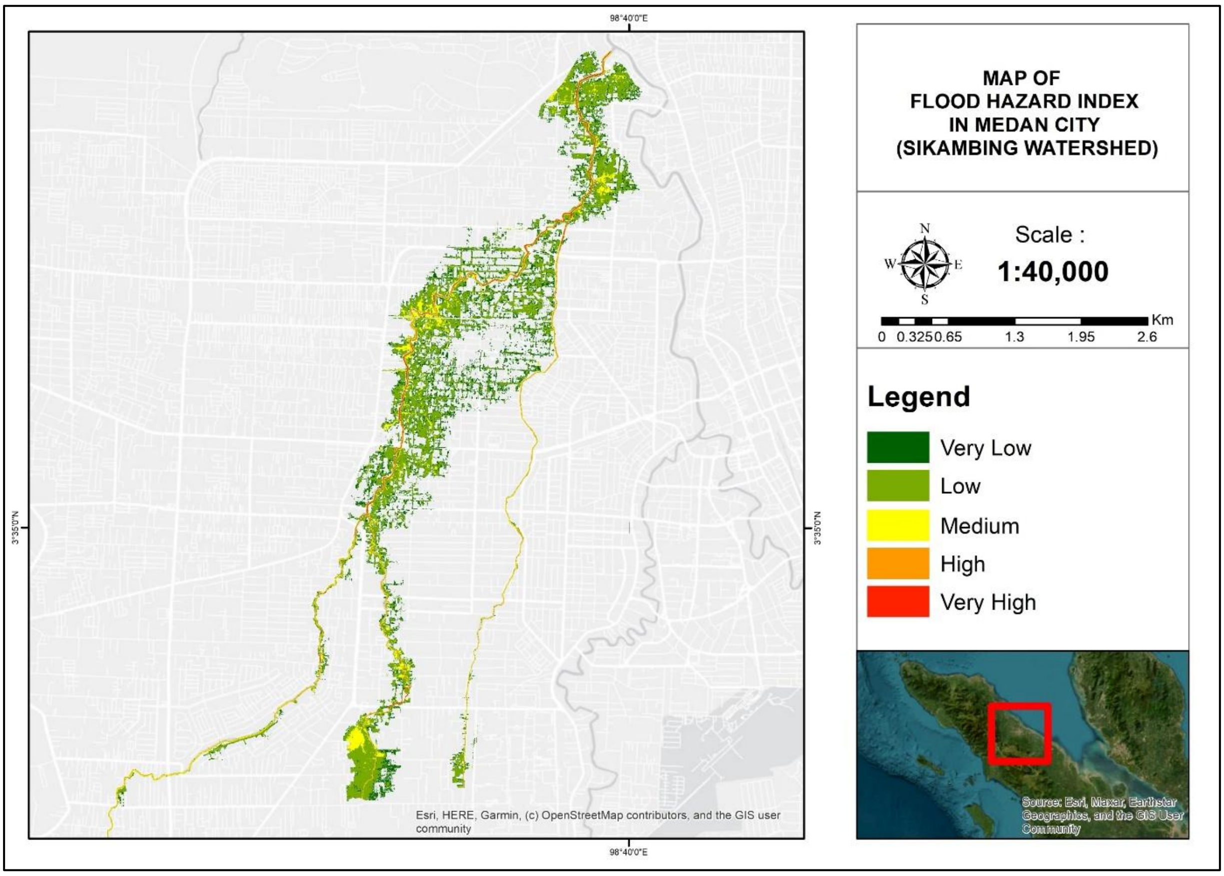

Figure 8 Flood hazard map based on modification parameters

Although the high and very high classifications have very small representations, the medium classification is present in several areas, covering 17.43 hectares, which represents 7.66% of the total inundated area.

Table 6 Flood hazard classification based on NDMA parameter

Flood Hazard Classification	Flood Inundation Area (ha)	Percentage (%)
Low	223,89	98.35
Medium	3,25	1.43
High	0.52	0.23
Total Area	227.65	100.00

Table 7 Flood hazard classification based on modification parameters

Flood Hazard Classification	Flood Inundation Area (ha)	Percentage (%)
Very Low	68.26	29.98
Low	141.87	62.32
Medium	17.43	7.66
High	0.09	0.04
Very High	0.00	0.00
Total Area	227.65	100.00

The comparison of flood hazard maps based on NDMA parameters and modified parameters reveals significant differences in the distribution of flood hazard classes. Although the total inundated area remains the same (227.65 hectares), the use of different parameters results in substantial changes in the proportions of each hazard class. The flood hazard map based on NDMA parameters is dominated by the low classification (98.35%), with only a small fraction of the area categorized as medium (1.43%) and high (0.23%). This indicates that relying solely on the depth parameter tends to yield a lower overall flood hazard assessment.

By incorporating depth and velocity (dv) parameters, as well as flood duration (T), the modified map demonstrates a more diverse distribution of hazard classes. While the low classification still predominates (62.32%), there is a significant increase in the area classified as medium (7.66%). Additionally, a very low classification (29.98%) emerges, which was absent in the previous map. The high and very high classifications, although small in area, are also identifiable in this analysis.

These differences in results can be directly attributed to the parameters used in each analysis. The NDMA parameters, which rely solely on depth, simplify the flood hazard assessment. In contrast, the modified parameters that combine depth (d), depth and velocity (dv), and flood duration (T) provide a more comprehensive understanding of flood hazards.

The mapping results also indicate that the depth and velocity parameters (dv) account for the energy of water flow, which correlates with potential damage. Flood duration (T) is also a critical factor, as prolonged inundation can lead to more severe impacts. By considering these factors, the modified parameters yield a more detailed flood hazard map that offers more accurate information for disaster mitigation planning. For instance, areas classified as medium in the modified map, despite having the same depth as those classified as low in the NDMA map, may possess a higher hazard potential due to the consideration of flow velocity or longer inundation duration. This distinction is crucial for evacuation planning and the development of flood control infrastructure.

CONCLUSIONS

This study demonstrates an improvement in flood hazard assessment that is more comprehensive compared to assessments based solely on depth (d) parameters. With the total inundated area remaining the same, the comparison of the generated flood hazard maps reveals significant differences in the distribution of hazard classes. The flood hazard assessment that integrates flood depth (d), flow depth and velocity (dv), and flood duration (T) results in a more detailed class distribution, with an increase in the area classified as medium that was previously undetected. This research is expected to contribute to the development of more effective flood mitigation policies. Furthermore, it is anticipated that future studies should consider the complexity of flood causative factors and integrate additional parameters to enhance the accuracy of flood hazard assessments and support more effective disaster management practices.

ACKNOWLEDGMENTS

The authors would like to express their deepest gratitude to the Ministry of Public Works of the Republic of Indonesia for the support and assistance provided during this research. We also extend our thanks to the Sumatra II River Basin Office in Medan for their support in providing the data necessary for the completion of this study.

REFERENCES

[1] Head of the National Disaster Management Agency of the Republic of Indonesia, ‘Peraturan Badan Nasional Penanggulangan Banjir No 7 Tahun 2022 tentang Rencana Nasional Penanggulangan Bencana Tahun 2020-2024’, 2022

[2] Head of the National Disaster Management Agency of the Republic of Indonesia, ‘Indeks Risiko Bencana Indonesia’, in *IRBI 2023 Indeks Risiko Bencana Indonesia*, National Disaster Management Agency of the Republic of Indonesia, 2023.

[3] H. Yosua, M. Syahril, B. Kusuma, and J. Nugroho, ‘An assessment of pluvial hazard in South Jakarta based on land-use/cover change from 2016 to 2022 An assessment of pluvial hazard in South Jakarta based on land-use/ cover change from 2016 to 2022’, *Front Built Environ*, 2024, doi: 10.3389/fbuil.2023.1345894/full.

[4] W. G. Bennett *et al.*, ‘Modelling compound flooding: a case study from Jakarta, Indonesia’, *Natural Hazards*, vol. 118, no. 1, pp. 277–305, Aug. 2023, doi: 10.1007/s11069-023-06001-1.

[5] H. Tabari, ‘Climate change impact on flood and extreme precipitation increases with water

availability', *Sci Rep*, vol. 10, no. 1, Dec. 2020, doi: 10.1038/s41598-020-70816-2.

[6] M. Bermúdez, J. F. Farfán, P. Willems, and L. Cea, 'Assessing the Effects of Climate Change on Compound Flooding in Coastal River Areas', *Water Resour Res*, vol. 57, no. 10, Oct. 2021, doi: 10.1029/2020WR029321.

[7] V. Daksiya, P. V. Mandapaka, and E. Y. M. Lo, 'Effect of climate change and urbanisation on flood protection decision-making', *J Flood Risk Manag*, vol. 14, no. 1, Mar. 2021, doi: 10.1111/jfr3.12681.

[8] M. Álvarez, J. Puertas, E. Peña, and M. Bermúdez, 'Two-dimensional dam-break flood analysis in data-scarce regions: The case study of Chipembe dam, Mozambique', *Water (Switzerland)*, vol. 9, no. 6, 2017, doi: 10.3390/w9060432.

[9] M. S. B. Kusuma, T. Setiawati, and M. Farid, 'Experimental model of dam break flow around several blockages configurations', *International Journal of GEOMATE*, vol. 16, no. 58, pp. 26–32, Jun. 2019, doi: 10.21660/2019.58.97684.

[10] M. Farid, B. Gunawan, M. S. Badri Kusuma, S. A. Habibi, and A. Yahya, 'Assessment of flood risk reduction in Bengawan Solo River: A case study of Sragen Regency', *International Journal of GEOMATE*, vol. 18, no. 70, pp. 229–234, 2020, doi: 10.21660/2020.70.18010.

[11] T. N. A. Kesuma, M. S. B. Kusuma, M. Farid, A. A. Kuntoro, and H. P. Rahayu, 'AN ASSESSMENT OF FLOOD HAZARDS DUE TO THE BREACH OF THE MANGGARAI FLOOD GATE', *International Journal of GEOMATE*, vol. 23, no. 95, pp. 104–111, Jul. 2022, doi: 10.21660/2022.95.3055.

[12] A. Maranzoni, M. D'Oria, and C. Rizzo, 'Quantitative flood hazard assessment methods: A review', Mar. 01, 2023, *John Wiley and Sons Inc*. doi: 10.1111/jfr3.12855.

[13] Head of the National Disaster Management Agency of the Republic of Indonesia, 'Peraturan Kepala Badan Nasional Penanggulangan Bencana Nomor 02 Tahun 2012 tentang Pedoman Umum Pengkajian Risiko Bencana', 2012

[14] G. P. Smith, E. K. Davey, and R. J. Cox, 'Flood hazard', 2014.

[15] F. Silvestro *et al.*, 'What if the 25 October 2011 event that struck Cinque Terre (Liguria) had happened in Genoa, Italy? Flooding scenarios, hazard mapping and damage estimation', *Natural Hazards and Earth System Sciences*, vol. 16, no. 8, pp. 1737–1753, Aug. 2016, doi: 10.5194/nhess-16-1737-2016.

[16] M. Vojtek and J. Vojteková, 'Flood hazard and flood risk assessment at the local spatial scale: a case study', *Geomatics, Natural Hazards and Risk*, vol. 7, no. 6, pp. 1973–1992, Nov. 2016, doi: 10.1080/19475705.2016.1166874.

[17] E. Psomiadis, L. Tomanis, A. Kavvadias, K. X. Soulis, N. Charizopoulos, and S. Michas, 'Potential dam breach analysis and flood wave risk assessment using HEC-RAS and remote sensing data: A multicriteria approach', *Water (Switzerland)*, vol. 13, no. 3, Feb. 2021, doi: 10.3390/w13030364.

[18] P. Mani, C. Chatterjee, and R. Kumar, 'Flood hazard assessment with multiparameter approach derived from coupled 1D and 2D hydrodynamic flow model', *Natural Hazards*, vol. 70, no. 2, pp. 1553–1574, Jan. 2014, doi: 10.1007/s11069-013-0891-8.

[19] N. Ongdas, F. Akiyanova, Y. Karakulov, A. Muratbayeva, and N. Zinabdin, 'Application of hec-ras (2d) for flood hazard maps generation for yesil (ishim) river in kazakhstan', *Water (Switzerland)*, vol. 12, no. 10, pp. 1–20, Oct. 2020, doi: 10.3390/w12102672.

[20] T. Tingsanchali and T. Promping, 'Comprehensive Assessment of Flood Hazard, Vulnerability, and Flood Risk at the Household Level in a Municipality Area: A Case Study of Nan Province, Thailand', *Water (Switzerland)*, vol. 14, no. 2, Jan. 2022, doi: 10.3390/w14020161.

[21] Minister of Public Works of the Republic of Indonesia, 'Peraturan Menteri Pekerjaan Umum Republik Indonesia Nomor 12/PRT/M/2014 Tentang Penyelenggaraan Sistem Drainase Perkotaan', 2014

[22] L. Cea and P. Costabile, 'Flood Risk in Urban Areas: Modelling, Management and Adaptation to Climate Change: A Review', Mar. 01, 2022, *MDPI*. doi: 10.3390/hydrology9030050.

[23] NDMA, 'Data Informasi Bencana Indonesia (DIBI)'. Accessed: Nov. 17, 2024. [Online]. Available: https://dibi.bnpb.go.id

[24] Minister of Public Works of the Republic of Indonesia, 'Keputusan Menteri Pekerjaan Umum Nomor 52/KPTS/M/2012 Tentang Pola Pengelolaan Sumber Daya Air Wilayah Sungai Belawan Ular Padang', 2012

[25] Minister of Public Works of the Republic of Indonesia, 'Peraturan Menteri Pekerjaan Umum dan Perumahan Rakyat Republik Indonesia Nomor 28/PRT/M/2015 tentang Penetapan Garis Sempadan Sungai dan Garis Sempadan Danau', 2015

[26] L. Milanesi, M. Pilotti, and R. Ranzi, 'A conceptual model of people's vulnerability to floods', *Water Resour Res*, vol. 51, no. 1, pp. 182–197, 2015, doi: 10.1002/2014WR016172.

[27] A. Luke *et al.*, 'Going beyond the flood insurance rate map: Insights from flood hazard map co-production', *Natural Hazards and Earth System Sciences*, vol. 18, no. 4, pp. 1097–1120, Apr. 2018, doi: 10.5194/nhess-18-1097-2018.

[28] P. Udmale, Y. Tachikawa, K. Kobayashi, and T. Sayama, 'Flood Hazard Mapping in Japan', in *Catalogue of Hydrologic Analysis for Asia and the Pacific Volume 1 Flood Hazard Mapping*, UNESCO, 2019, pp. 17–37.

[29] F. Guillier, 'French Insurance and Flood Risk: Assessing the Impact of Prevention Through the Rating of Action Programs for Flood Prevention', *International Journal of Disaster Risk Science*, vol. 8, no. 3, pp. 284–295, Sep. 2017, doi: 10.1007/s13753-017-0140-y.

[30] International Commission for the Protection of the Rhine (ICPR), 'International flood risk management plan for the International River Basin District "Rhine" (Part A) (catchment areas > 2.500 km^2)', International Commission for the Protection of the Rhine (ICPR), 2021. [Online]. Available: www.iksr.org

[31] Head of the National Standardization Agency of the Republic of Indonesia, 'SNI 2451:2016 Tata Cara Perhitungan Debit Banjir Rencana', 2016 [Online]. Available: www.bsn.go.id

[32] Minister of Public Works of the Republic of Indonesia, 'Petunjuk Teknis Perhitungan Debit Banjir Pada Bendungan', 2017

[33] X. Wang and H. Bi, 'The effects of rainfall intensities and duration on SCS-CN model parameters under simulated rainfall', *Water (Switzerland)*, vol. 12, no. 6, Jun. 2020, doi: 10.3390/W12061595.

[34] M. Sharifi, M. R. M. Tabatabai, and S. H. G. Najafabadi, 'Determination of river design discharge (Tar river case study)', *Journal of Water and Climate Change*, vol. 12, no. 2, pp. 612–626, Mar. 2021, doi: 10.2166/wcc.2020.278.

[35] K. Naito and G. Parker, 'Can Bankfull Discharge and Bankfull Channel Characteristics of an Alluvial Meandering River be Cospecified From a Flow Duration Curve?', *J Geophys Res Earth Surf*, vol. 124, no. 10, pp. 2381–2401, Oct. 2019, doi: 10.1029/2018JF004971.

[36] Minister of Public Works of Indonesia, 'Peraturan Menteri Pekerjaan Umum dan Perumahan Rakyat Republik Indonesia Nomor 5 Tahun 2021 tentang Petunjuk Operasional Pengelolaan Dana Alokasi Khusus Infrastruktur Pekerjaan Umum dan Perumahan Rakyat', 2021

[37] S. A. Djafri, S. Cherhabil, M. A. Hafnaoui, and M. Madi, 'Flood modeling using HEC-RAS 2D and IBER 2D: a comparative study', *Water Supply*, Sep. 2024, doi: 10.2166/ws.2024.184.

[38] Y. Z. Kaya and F. Üneş, 'Comparison of three different satellite data on 2D flood modeling using HEC-RAS (5.0.7) software and investigating the improvement ability of the RAS Mapper tool', *J Flood Risk Manag*, vol. 18, no. 1, Mar. 2025, doi: 10.1111/jfr3.13046.

[39] A. Mihu-Pintilie, C. I. Cîmpianu, C. C. Stoleriu, M. N. Pérez, and L. E. Paveluc, 'Using high-density LiDAR data and 2D streamflow hydraulic modeling to improve urban flood hazard maps: A HEC-RAS multi-scenario approach', *Water (Switzerland)*, vol. 11, no. 9, 2019, doi: 10.3390/w11091832.

[40] B. Kim, B. F. Sanders, J. E. Schubert, and J. S. Famiglietti, 'Mesh type tradeoffs in 2D hydrodynamic modeling of flooding with a Godunov-based flow solver', *Adv Water Resour*, vol. 68, pp. 42–61, 2014, doi: 10.1016/j.advwatres.2014.02.013.

[41] C. Mattas, D. Karpouzos, P. Georgiou, and T. Tsapanos, 'Two-Dimensional Modelling for Dam Break Analysis and Flood Hazard Mapping: A Case Study of Papadia Dam, Northern Greece', *Water (Switzerland)*, vol. 15, no. 5, Mar. 2023, doi: 10.3390/w15050994.

[42] Z. Liu, V. Merwade, and K. Jafarzadegan, 'Investigating the role of model structure and surface roughness in generating flood inundation extents using one- and two-dimensional hydraulic models', *J Flood Risk Manag*, vol. 12, no. 1, Mar. 2019, doi: 10.1111/jfr3.12347.

[43] K. Vashist and K. K. Singh, 'HEC-RAS 2D modeling for flood inundation mapping: a case study of the Krishna River Basin', *Water Pract Technol*, vol. 18, no. 4, pp. 831–844, Apr. 2023, doi: 10.2166/wpt.2023.048.

[44] G. W. Brunner, C. T. Ackerman, and C. R. Goodell, 'HEC-RAS River Analysis System HEC-RAS User's Manual Version 6.5', 2024.

[45] M. Muthusamy, M. R. Casado, G. Salmoral, T. Irvine, and P. Leinster, 'A remote sensing based integrated approach to quantify the impact of fluvial and pluvial flooding in an urban catchment', *Remote Sens (Basel)*, vol. 11, no. 5, Mar. 2019, doi: 10.3390/rs11050577.

[46] Chairman NDMA of Pakistan, 'NDMA Policy Guidelines For Conduct of Multi Hazard Vulnerability And Risk Assessment (MHVRA)', 2016

[47] N. H. bin Ghazali and S. bin Osman, 'Flood Hazard Mapping in Malaysia Case Study Sg. Kelantan River Basin', in *Catalogue of Hydrologic Analysis for Asia and the Pacific Volume 1 Flood Hazard Mapping*, UNESCO, 2019, pp. 54–80.

[48] J.-H. Lee, Y. Seo, S.-S. Park, and H.-S. Cho, 'Flood Hazard Map of Korea', in *Catalogue of Hydrologic Analysis for Asia and the Pacific Volume 1 Flood Hazard Mapping*, UNESCO, 2019, pp. 38–53.

[49] M. A. Al Baky, M. Islam, and S. Paul, 'Flood Hazard, Vulnerability and Risk Assessment for Different Land Use Classes Using a Flow Model', *Earth Systems and Environment*, vol. 4, no. 1, pp. 225–244, Mar. 2020, doi: 10.1007/s41748-019-00141-w.

[50] B. Evans, A. S. Chen, S. Djordjević, J. Webber, A. G. Gómez, and J. Stevens, 'Investigating the effects of pluvial flooding and climate change on traffic flows in barcelona and bristol', *Sustainability (Switzerland)*, vol. 12, no. 6, Mar. 2020, doi: 10.3390/su12062330.

[51] W. C. Liu, T. H. Hsieh, and H. M. Liu, 'Flood risk assessment in urban areas of southern Taiwan', *Sustainability (Switzerland)*, vol. 13, no. 6, Mar. 2021, doi: 10.3390/su13063180.

[52] M. Kramer, K. Terheiden, and S. Wieprecht, 'Safety criteria for the trafficability of inundated roads in urban floodings', *International Journal of Disaster Risk Reduction*, vol. 17, pp. 77–84, Aug. 2016, doi: 10.1016/j.ijdrr.2016.04.003.

[53] Federal Minister for Sustainability and Tourism of Austria, 'Flood Risk Management in Austria', 2018.

[54] B. Handyastono, E. O. Nugroho, M. R. S. Kasim, F. J. Fachri, A. Rianto, and M. Hazmi, 'Modification of Flood Hazard Assessment in

Pemaluan River: Case Study of Pemaluan Village, Penajam Paser Utara Regency', *IOP Conf Ser Earth Environ Sci*, vol. 1416, no. 1, p. 012028, Dec. 2024, doi: 10.1088/1755-1315/1416/1/012028.